

# Design, Synthesis, and Evaluation of 9-D-Ribityl-1,3,7-trihydro-2,6,8-purinetrione, a Potent Inhibitor of Riboflavin Synthase and Lumazine Synthase

Mark Cushman,<sup>\*,†</sup> Donglai Yang,<sup>†</sup> Klaus Kis,<sup>‡</sup> and Adelbert Bacher<sup>‡</sup>

Department of Medicinal Chemistry and Molecular Pharmacology, School of Pharmacy and Pharmacal Sciences, Purdue University, West Lafayette, Indiana 47907, and Lehrstuhl für Organische Chemie und Biochemie, Technische Universität München, D-85747 Garching, Germany

cushman@pharmacy.purdue.edu

Received July 13, 2001

Reduction of 5-nitro-6-D-ribitylaminouracil (**9**) afforded 5-amino-6-D-ribitylaminouracil (**1**), which reacted with ethyl chloroformate to yield 5-ethylcarbamoyl-6-D-ribitylaminouracil (**12**). The latter compound was cyclized to 9-D-ribityl-1,3,7-trihydropurine-2,6,8-trione (**13**), which was found to be a relatively potent inhibitor of both *Escherichia coli* riboflavin synthase ( $K_i$  0.61  $\mu$ M) and *Bacillus subtilis* lumazine synthase ( $K_i$  46  $\mu$ M). Molecular modeling of the lumazine synthase–inhibitor complex indicated the possibility for hydrogen bonding between the Lys135  $\epsilon$ -amino group of the enzyme and both the 8-keto group and the 4'-hydroxyl group of the ligand. A bisubstrate analogue of the riboflavin synthase-catalyzed reaction, 1,4-bis[1-(9-D-ribityl)-1,3,7-trihydropurine-2,6,8-trionyl]-butane (**18**), was also synthesized using a similar route and was found to be inactive as an inhibitor of both riboflavin synthase and lumazine synthase.

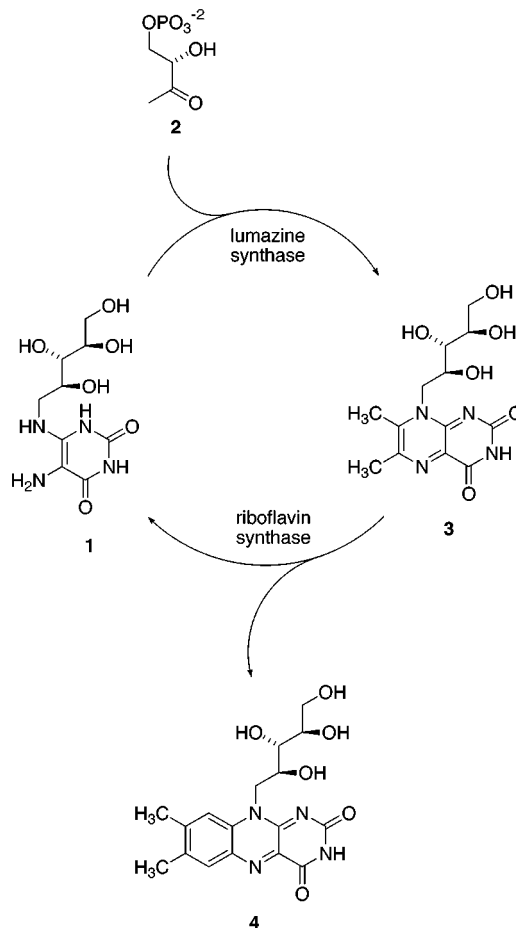
## Introduction

Riboflavin synthase catalyzes an unusual dismutation reaction in which a four-carbon unit is transferred from one molecule of 6,7-dimethyl-8-D-ribityllumazine (**3**), bound at the donor site of the enzyme, to a second molecule of **3**, bound at the acceptor site of the enzyme, resulting in the formation of one molecule of riboflavin (**4**) and one molecule of the pyrimidinedione **1** (Scheme 1).<sup>1–5</sup> In an efficient recycling reaction, lumazine synthase catalyzes the condensation of the pyrimidinedione **1** with the four-carbon unit **2**, resulting in the substrate **3** used by riboflavin synthase.<sup>6</sup>

A plausible mechanistic pathway for the lumazine synthase-catalyzed reaction involves an initial Schiff base formation between the ketone **2** and the primary amine **1**, resulting in the imine **5**, which eliminates phosphate to form the enol **6** (Scheme 2). Tautomerization of the enol **6** to the ketone **7**, followed by the addition of the secondary amino group to the ketone, leads to the formation of the covalently hydrated lumazine **8**. Elimination of water yields the observed product **3**.

The X-ray structure of a reconstituted, icosahedral  $\beta_{60}$  *Bacillus subtilis* lumazine synthase capsid complexed

Scheme 1



with the substrate analogue **9** has allowed the construction of a hypothetical model of the phosphate **5** bound in the active site.<sup>7</sup> The model has also been substantiated

\* Ph: 765-494-1465. Fax: 765-494-6790.

<sup>†</sup> Purdue University.

<sup>‡</sup> Technische Universität München.

(1) Plaut, G. W. E.; Smith, C. M.; Alworth, W. L. *Annu. Rev. Biochem.* **1974**, *43*, 899–922.

(2) Plaut, G. W. E. In *Comprehensive Biochemistry*; Florkin, M., Stotz, E. H., Eds.; Elsevier: Amsterdam, 1971; Vol. 21, pp 11–45.

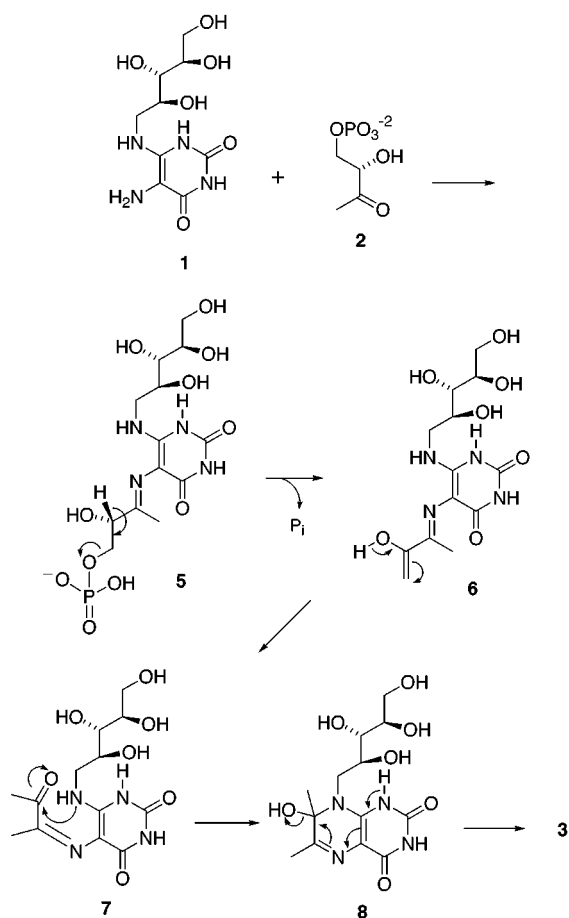
(3) Beach, R. L.; Plaut, G. W. E. *J. Am. Chem. Soc.* **1970**, *92*, 2913–2916.

(4) Bacher, A.; Eberhardt, S.; Richter, G. In *Escherichia coli and Salmonella: Cellular and Molecular Biology*, 2nd ed.; Neidhardt, F. C., Ed.; ASM Press: Washington, DC, 1996; pp 657–664.

(5) Bacher, A.; Fischer, M.; Kis, K.; Kugelbrey, K.; Mörtl, S.; Scheuring, J.; Weinkauff, S.; Eberhardt, S.; Schmidt-Bäse, K.; Huber, R.; Ritsert, K.; Cushman, M.; Ladenstein, R. *Biochem. Soc. Trans.* **1996**, *24*, 89–94.

(6) Volk, R.; Bacher, A. *J. Am. Chem. Soc.* **1988**, *110*, 3651–3653.

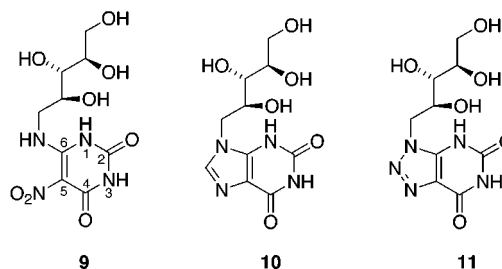
Scheme 2



by a crystal structure of a phosphonate analogue of **5** bound to *Saccharomyces cerevisiae* lumazine synthase.<sup>8,9</sup> The placement of the phosphate group of **5** in the model of the complex was accomplished by overlapping it with an inorganic phosphate that had been incorporated from the solvent during crystallization of the complex of **9** with the enzyme for X-ray structure determination. The geometry of the enzyme-bound imine in **5** is not established, and both the *E*- and the *Z*-imines can be modeled in the active site of lumazine synthase reasonably well, with the phosphate and pyrimidine ring overlapping with the pyrimidine ring of an inorganic phosphate present in the crystal structure of bound **9**. However, a *Z*-imine is required in intermediate **7** in order for cyclization to occur. The details of the conformational change of the side chain in the conversion of **5** (or its *Z*-isomer) to **7** have not been defined. Since the phosphate is not near the amino group, an extensive conformational reorganization of the side chain must occur after phosphate elimination from **5** in order to allow the ketone to be brought into close proximity with the amine so the cyclization can occur.

Certain Gram-negative bacteria, including *Escherichia coli* and *Salmonella typhimurium*, lack an efficient riboflavin uptake system and are therefore dependent on endogenous synthesis.<sup>10,11</sup> More specifically, it has been

shown that riboflavin-deficient mutants of both of these bacteria require riboflavin concentrations well above 10 mg/L of culture medium. Similar concentrations of riboflavin are also required to support the growth of riboflavin-deficient mutants of the yeasts *Candida guilliermondii* and *S. cerevisiae*.<sup>12–14</sup> These observations support the idea that the enzymes involved in riboflavin biosynthesis are rational targets for the development of antibiotics to treat Gram-negative bacterial and yeast infections.



A collaborative effort between our research groups has resulted in the design and synthesis of a number of riboflavin synthase and lumazine synthase inhibitors.<sup>8,15–20</sup> These included 2,6-dioxo-(1*H*,3*H*)-9-*N*-ribitylpyrimidine-2,6,8-trione (**10**) and 2,6-dioxo-(1*H*,3*H*)-8-aza-9-*N*-ribitylpyrimidine-2,6,8-trione (**11**).<sup>20</sup> When tested as an inhibitor of riboflavin synthase, the purine **10** displayed a *K<sub>i</sub>* of 540  $\mu$ M, and the azapurine **11** resulted in a *K<sub>i</sub>* of 390  $\mu$ M. On the other hand, versus lumazine synthase, the purine **10** had a *K<sub>i</sub>* of 470  $\mu$ M and the azapurine produced a *K<sub>i</sub>* of 330  $\mu$ M. In considering the relative activities of **10** and **11** versus lumazine synthase, it was proposed that the greater potency of the azapurine **11** might possibly reflect an electrostatic and/or hydrogen bonding interaction between the side chain amino group of Lys135 of the enzyme and the N-8 nitrogen of **11**, which would not be possible with **10**. This interpretation has led to the consideration of other systems that might more effectively target Lys135, including 9-D-ribose-1,3,7-trihydro-2,6,8-trione (**13**). On the basis of molecular modeling, the 8-keto group of **13** seemed to be ideally positioned to hydrogen bond with the side chain amino group of Lys135.

## Results and Discussion

The synthesis of the desired compound **13** is outlined in Scheme 3. Catalytic hydrogenation of 5-nitro-6-ribitylaminouracil (**9**)<sup>21</sup> over palladium on charcoal afforded

(7) Ritsert, K.; Huber, R.; Turk, D.; Ladenstein, R.; Schmidt-Bäse, K.; Bacher, A. *J. Mol. Biol.* **1995**, *253*, 151–167.

(8) Cushman, M.; Mihalic, J. T.; Kis, K.; Bacher, A. *J. Org. Chem.* **1999**, *64*, 3838–3845.

(9) Meining, W.; Mörtl, S.; Fischer, M.; Cushman, M.; Bacher, A.; Ladenstein, R. *J. Mol. Biol.* **2000**, *299*, 181–197.

(10) Bandrin, S. V.; Beburow, M. Y.; Rabinovich, P. M.; Stepanov, A. I. *Genetika* **1979**, *15*, 2063–2065.

(11) Wang, A. I. *Chuan Hsueh Pao* **1992**, *19*, 362–368.

(12) Oltmanns, O.; Lingens, F. Z. *Naturforschung* **1967**, *22*, 751–754.

(13) Logvinenko, E. M.; Shavlovsky, G. M. *Mikrobiologiya* **1967**, *41*, 978–979.

(14) Roberts, J. C.; Gao, H.; Gopalsami, A.; Kongsjahju, A.; Patch, R. J. *Tetrahedron Lett.* **1997**, *38*, 355–358.

(15) Cushman, M.; Patrick, D. A.; Bacher, A.; Scheuring, J. *J. Org. Chem.* **1991**, *56*, 4603–4608.

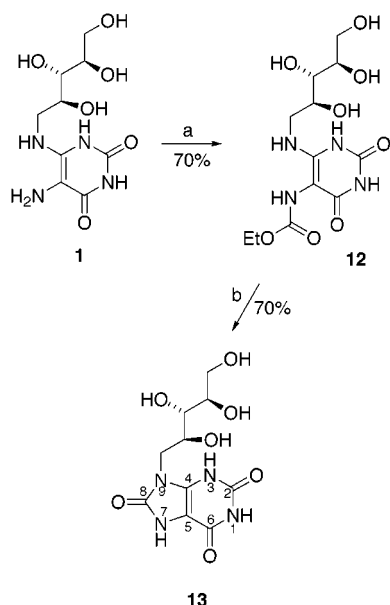
(16) Cushman, M.; Patel, H. H.; Scheuring, J.; Bacher, A. *J. Org. Chem.* **1992**, *57*, 5630–5643.

(17) Cushman, M.; Patel, H. H.; Scheuring, J.; Bacher, A. *J. Org. Chem.* **1993**, *58*, 4033–4042.

(18) Cushman, M.; Mavandadi, F.; Yang, D.; Kugelbrey, K.; Kis, K.; Bacher, A. *J. Org. Chem.* **1999**, *64*, 4635–4642.

(19) Cushman, M.; Mavandadi, F.; Kugelbrey, K.; Bacher, A. *J. Org. Chem.* **1997**, *62*, 8944–8947.

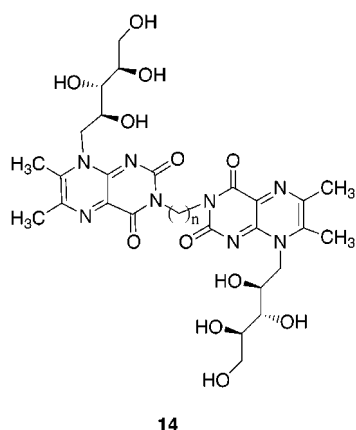
(20) Cushman, M.; Mavandadi, F.; Kugelbrey, K.; Bacher, A. *Bioorg. Med. Chem.* **1998**, *6*, 409–415.

Scheme 3<sup>a</sup>

<sup>a</sup> Reagents and conditions: (a) ClCOOEt, Et<sub>3</sub>N, aq CH<sub>3</sub>CN, 23 °C (10 h); (b) NaOEt, EtOH, reflux (24 h).

the unstable amino compound **1**.<sup>15</sup> Since intermediate **1** is extremely sensitive to oxidation, leading to a multitude of products, it was treated in situ in the hydrogenation reaction mixture with ethyl chloroformate. After the reaction was complete, the catalyst was removed by filtration and the desired 5-ethylcarbamoyl-6-ribitylaminouracil (**12**) was isolated from the filtrate. Cyclization of **12** was then carried out with sodium ethoxide in refluxing ethanol to afford the desired product **13**.

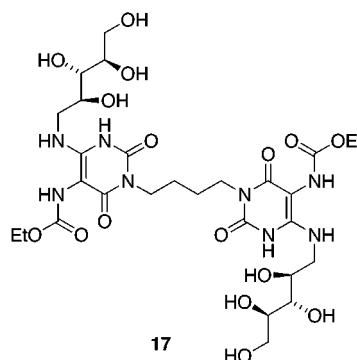
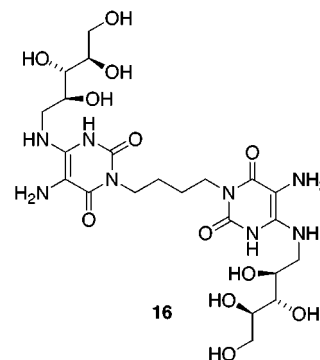
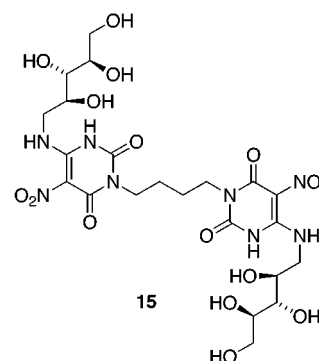
The dismutation reaction catalyzed by riboflavin synthase requires the presence of two substrate molecules, or derivatives thereof, to be bound in the active site of the enzyme at the same time.<sup>3,22,23</sup> In an attempt to prepare bisubstrate inhibitors of riboflavin synthase, a series of bis(lumazines) of general structure **14** were



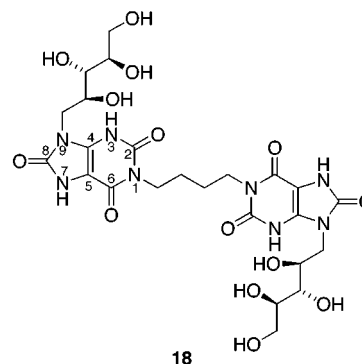
therefore previously prepared and tested as inhibitors of riboflavin synthase.<sup>18</sup> Maximal activity was found in the bis(lumazine) in which the linker chain connecting the two substrate molecules was a straight chain containing

four carbon atoms (structure **14**,  $n = 4$ ). This suggests that a similar bis(purinetrione) might also be an effective inhibitor of riboflavin synthase. Accordingly, the desired 1,4-bis[1-(9-D-ribityl-1,3,7-trihydropurine-2,6,8-trionyl)]-butane (**18**) was synthesized.

The synthesis of **18** proceeded through intermediates **15**, **16**, and **17**, and was carried out using the methodol-



ogy outlined for the monomer **13** in Scheme 3. In contrast to the riboflavin synthase inhibitory activity seen with the bis(lumazine) **14** ( $n = 4$ ) ( $K_i = 37 \mu\text{M}$ ), the bis(purinetrione) **18** proved to be inactive as a riboflavin



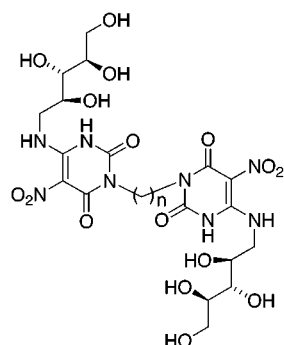
(21) Cresswell, R. M.; Wood, H. S. C. *J. Chem. Soc.* **1960**, 4768–4775.

(22) Otto, M.; Bacher, A. *Eur. J. Biochem.* **1981**, *115*, 511–517.

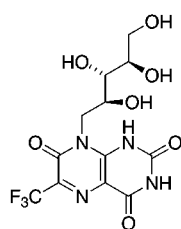
(23) Scheuring, J.; Fischer, M.; Cushman, M.; Lee, J.; Bacher, A.; Oschkinat, H. *Biochemistry* **1996**, *35*, 9637–9646.

synthase inhibitor, and it was also inactive versus lumazine synthase (Table 1). Evidently, the bisubstrate inhibitor approach requires lumazines very close in structure to the natural substrate to be effective with riboflavin synthase.

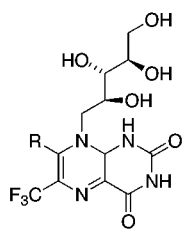
The purinetriene **13** was tested for inhibition of lumazine synthase  $\beta_{60}$  capsids and recombinant riboflavin synthase from *E. coli*. The resulting Lineweaver–Burk plots are shown in Figure 1, and the inhibition constants and types of inhibition displayed by **13** are listed in Table 1, together with the results from previously synthesized riboflavin synthase and lumazine synthase inhibitors.<sup>8,15–20</sup>



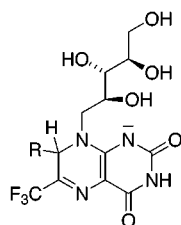
**15a** ( $n = 3$ )  
**15b** ( $n = 5$ )



**20**



**21**  $R = \text{CH}_3$   
**22**  $R = \text{H}$

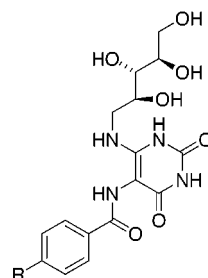


**23**  $R = \text{SO}_3^-$   
**24**  $R = \text{S}^-$   
**25**  $R = \text{SCH}_2\text{CH}_2\text{OH}$   
**26**  $R = \text{SCH}_2\text{CHOHC HOCH}_2\text{S}^-$   
**27**  $R = \text{SCH}_2\text{CH}(\text{NH}_2)\text{COO}^-$

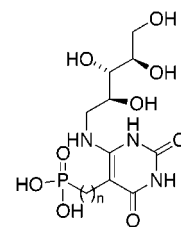
Different kinetic models were considered, and the most likely inhibition mechanisms for **13** were found to be partial inhibition for lumazine synthase and strictly competitive inhibition for riboflavin synthase. The  $K_i$  of 0.61  $\mu\text{M}$  observed for 3-D-ribityl-2,6,8-purinetrione (**13**) makes it the most potent *E. coli* riboflavin synthase inhibitor ever reported. Its  $K_i$  of 46  $\mu\text{M}$  versus the *B. subtilis* lumazine synthase, along with that of 43  $\mu\text{M}$  presently determined for the synthetic intermediate **9**, rate these two compounds as the most potent lumazine synthase inhibitors described to date.

The crystal structure of *E. coli* riboflavin synthase containing selenomethionine residues has been pub-

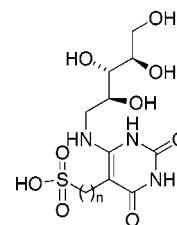
lished, and it might be possible to explain the high potency of **13** versus riboflavin synthase in structural terms when the coordinates become available.<sup>24</sup> A great deal is also known about the structure of lumazine synthase as a result of the availability of a 2.4 Å resolution X-ray structure of the substrate analogue **9** complexed with *B. subtilis* lumazine synthase.<sup>7</sup> In addition, the related 1.85 Å resolution X-ray structure of the phosphonate inhibitor **31b**<sup>8</sup> ( $K_i$  180  $\mu\text{M}$  versus *B. subtilis* lumazine synthase) bound to *S. cerevisiae*



**28**  $R = \text{SO}_2\text{F}$   
**29**  $R = \text{SO}_3\text{Na}$   
**30**  $R = \text{COCH}_2\text{CH}_2\text{CH}_2\text{COOH}$



**31a**  $n = 4$   
**31b**  $n = 5$   
**31c**  $n = 6$



**32a**  $n = 4$   
**32b**  $n = 5$   
**32c**  $n = 6$

lumazine synthase has also been published,<sup>9</sup> and its homologue **31c** has been docked in the active site of *B. subtilis* lumazine synthase by computer graphics molecular modeling.<sup>8</sup> The modeled structure of **31c** in complex with the enzyme was in close agreement with that of **31b**, which was later determined by X-ray crystallography.<sup>8,9</sup> These structures might allow a possible explanation of the high potency of **13** versus lumazine synthase. Accordingly, a molecular model was constructed by overlapping the structure of **13** with the structure of **9** in the active site of *B. subtilis* lumazine synthase. The structure of **9** was then removed, and the energy of the complex was minimized using the MMRR94 force field while allowing the ligand and the hydrated protein structure contained within a 6 Å sphere surrounding the ligand to remain flexible with the remainder of the protein structure frozen. The 6 Å flexible sphere surrounding the ligand was employed in order to allow for an induced fit of the ligand to the protein. The resulting Figure 2 was constructed by displaying the amino acid residues and one water molecule calculated to be involved in hydrogen bonding with the ligand **13**.

According to the model in Figure 2, the 8-keto group of **13** can hydrogen bond with the  $\epsilon$ -amino group of Lys135, which positions the 4'-hydroxyl group of the

(24) Liao, D.-I.; Wawrzak, Z.; Calabrese, J. C.; Viitanen, P. V.; Jordan, D. B. *Structure* **2001**, 9, 399–408.

Table 1. Inhibition Constants versus Lumazine Synthase and Riboflavin Synthase

compound	$K_i$ ( $\mu\text{M}$ )	
	lumazine synthase <sup>a</sup>	riboflavin synthase <sup>b</sup>
<b>4</b>		200
<b>9</b>	43.4 $\pm$ 4.1 ( $K_i$ , partial inhibition) 40 $\pm$ 2.8 ( $K_s$ ) 250 $\pm$ 47 ( $K_{is}$ ) <sup>c</sup> 79.2 $\pm$ 2 (kcat) 16 $\pm$ 33 (kcat')	120
<b>10</b>	470 <sup>c</sup>	540 <sup>c</sup>
<b>11</b>	330 <sup>c</sup>	390 <sup>c</sup>
<b>12</b>	>1000	>1000
<b>13</b>	46 $\pm$ 5 ( $K_i$ , partial inhibition) 250 $\pm$ 42 ( $K_{is}$ ) <sup>d</sup>	0.61 $\pm$ 0.05 ( $K_i$ , competitive inhibition) 9.6 $\pm$ 0.9 ( $K_s$ ) 39.9 $\pm$ 0.7 (kcat)
<b>14</b> ( $n = 3$ )	840 $\pm$ 490 ( $K_i$ , partial inhibition) <sup>e</sup> 2200 $\pm$ 660 ( $K_{is}$ ) <sup>e</sup>	320 $\pm$ 470 ( $K_i$ , partial inhibition) <sup>e</sup> 300 $\pm$ 30 ( $K_{is}$ ) <sup>e</sup>
<b>14</b> ( $n = 4$ )	>1000 <sup>e</sup>	37 $\pm$ 30 ( $K_i$ , mixed inhibition) <sup>f</sup> 57 $\pm$ 12 ( $K_{is}$ ) <sup>e</sup>
<b>14</b> ( $n = 5$ )	>1000 <sup>e</sup>	>1000 <sup>e</sup>
<b>15</b>	3700 <sup>e</sup>	3000 <sup>e</sup>
<b>15a</b>	5000 <sup>e</sup>	280 <sup>e</sup>
<b>15b</b>	1500 <sup>e</sup>	670 <sup>e</sup>
<b>17</b>	>1000	>1000
<b>18</b>	>1000	>1000
<b>19</b> (epimer A)		120 (pH 7.4) <sup>g</sup>
<b>19</b> (epimer A)		38 (pH 6.8) <sup>g</sup>
<b>20</b>		55 <sup>g</sup>
<b>21</b>		75 <sup>g</sup>
<b>22</b>		58 <sup>h</sup>
<b>23</b>		70 <sup>h</sup>
<b>24</b>		17 <sup>h</sup>
<b>25</b>		17 <sup>h</sup>
<b>26</b>		15
<b>27</b>		20 <sup>h</sup>
<b>28</b>	200 <sup>i</sup>	
<b>29</b>	360 <sup>i</sup>	
<b>30</b>	430 <sup>i</sup>	
<b>31a</b>	440 $\pm$ 200 ( $K_i$ , mixed inhibition) <sup>j</sup> 640 $\pm$ 300 ( $K_{is}$ ) <sup>j</sup>	>1000 <sup>j</sup>
<b>31b</b>	180 $\pm$ 88 ( $K_i$ , mixed inhibition) <sup>j</sup> 350 $\pm$ 22 ( $K_{is}$ ) <sup>j</sup>	>1000 <sup>j</sup>
<b>31c</b>	130 $\pm$ 33 ( $K_i$ , mixed inhibition) <sup>j</sup> 140 $\pm$ 15 ( $K_{is}$ ) <sup>j</sup>	>1000 <sup>j</sup>
<b>32a</b>	290 $\pm$ 120 ( $K_i$ , competitive inhibition) <sup>j</sup>	
<b>32b</b>	690 $\pm$ 290 ( $K_i$ , mixed inhibition) <sup>j</sup> 1500 $\pm$ 640 ( $K_{is}$ ) <sup>j</sup>	>1000 <sup>j</sup>
<b>32c</b>	290 $\pm$ 130 ( $K_i$ , mixed inhibition) <sup>j</sup> 580 $\pm$ 170 ( $K_{is}$ ) <sup>j</sup>	>1000 <sup>j</sup>

<sup>a</sup> Recombinant  $\beta_{60}$  capsids from *B. subtilis*. <sup>b</sup> Recombinant riboflavin synthase from *E. coli*. <sup>c</sup> Reference 20. <sup>d</sup>  $K_{is}$  is the equilibrium constant for the reaction  $\text{EI} + \text{S} \rightleftharpoons \text{EIS}$ . <sup>e</sup> Reference 18. <sup>f</sup> Strictly speaking, the data observed for bis(lumazine) **14** ( $n = 4$ ) cannot be interpreted in terms of any simple inhibition type, but it is most consistent with mixed type inhibition. <sup>g</sup> Reference 16. <sup>h</sup> Reference 17. <sup>i</sup> Reference 19. <sup>j</sup> Reference 8.

ligand to also accept a hydrogen bond from  $\epsilon$ -amino group of Lys135. Similar contacts are not made when the nitro compound **9** binds to the enzyme.<sup>7</sup> The  $K_d$  for compound **9** versus the lumazine synthase of *B. subtilis* was previously estimated to be 650 nM.<sup>25</sup> When tested as an inhibitor of *B. subtilis* lumazine synthase for direct comparison with **13**, compound **9** produced a  $K_i$  of 43  $\mu\text{M}$ . A comparison of the computer-generated hydrogen bonding patterns calculated for the binding of **13** to lumazine synthase with that resulting from the X-ray structure of **9** bound to lumazine synthase is shown in Figure 3. Although the inhibitor **9** does not hydrogen bond to Lys135, the hydrogen bonds between its 5'-hydroxyl group and Phe113, as well as its 2'-hydroxyl group and Phe57, are within the normal range for hydrogen bonding (N to O distances 3.1 and 2.9 Å, respectively), as compared to the corresponding distances calculated for

**13** of 4.1 and 4.1 Å, which are outside of the normal hydrogen bonding lengths. These factors seem to balance out, resulting in similar enzyme inhibitory potencies. Another difference between the two structures is that Glu58 in **9** hydrogen bonds with the 3'-hydroxyl group of the ligand, whereas in **13**, it is calculated to hydrogen bond with the 2'-hydroxyl group.

In contrast to the situation with lumazine synthase, the purinetriene **13** ( $K_i$  0.61  $\mu\text{M}$ ) is a much more potent inhibitor of *E. coli* riboflavin synthase than the nitropyrimidine **9** ( $K_i$  120  $\mu\text{M}$ ).<sup>20</sup> These differences in riboflavin synthase inhibitory activity can possibly be rationalized in the future when the crystal coordinates of riboflavin synthase are published.<sup>24</sup>

To place the activity of the purinetriene **13** in perspective, a complete listing of the inhibitory activities of all of the known *B. subtilis* lumazine synthase inhibitors and *E. coli* riboflavin synthase inhibitors has been provided in Table 1.<sup>8,15–20</sup> The  $K_i$  of 0.61  $\mu\text{M}$  observed for **13** versus

(25) Bacher, A.; Ludwig, H. C. *Eur. J. Biochem.* **1982**, *127*, 539–545.



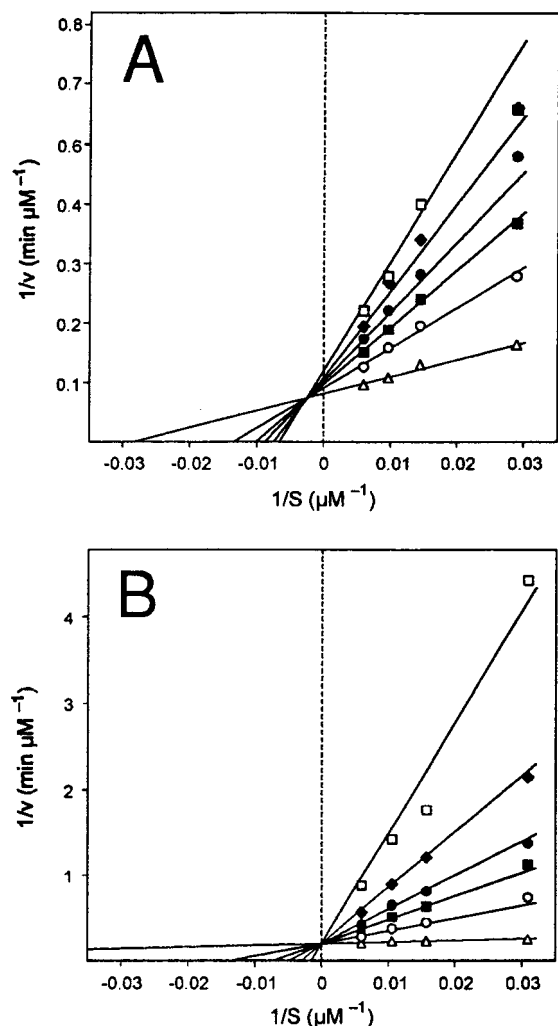


**Figure 1.** Lineweaver–Burk plots of the inhibition of lumazine synthase and riboflavin synthase by compound **13**. (A) Lumazine synthase. The concentration of the substrate **2** ranges from 17 to 166  $\mu\text{M}$ . Inhibitor concentrations:  $\square$ , 862;  $\blacklozenge$ , 431;  $\bullet$ , 259;  $\blacksquare$ , 172;  $\circ$ , 86;  $\triangle$ , 0  $\mu\text{M}$ . (B) Riboflavin synthase. The concentration of the substrate **3** ranged from 17 to 166  $\mu\text{M}$ . Inhibitor concentrations:  $\square$ , 40;  $\blacklozenge$ , 20;  $\bullet$ , 12;  $\blacksquare$ , 8;  $\circ$ , 4;  $\triangle$ , 0  $\mu\text{M}$ . The initial velocities of product formation,  $v$ , were determined at steady-state conditions with varying amounts of substrate,  $s$ , and inhibitor. The kinetic data were fitted with a nonlinear regression method using the program DynaFit from P. Kuzmic.<sup>27</sup> Different kinetic models were considered. The most likely inhibition mechanisms found were partial inhibition for lumazine synthase and strictly competitive inhibition for riboflavin synthase.

riboflavin synthase is significantly lower than that observed for the nearest-ranking compound, the D,L-dithiothreitol adduct **26** ( $K_i$  15  $\mu\text{M}$ ). Likewise, both **9** ( $K_i$  = 43  $\mu\text{M}$ ) and **13** ( $K_i$  = 46  $\mu\text{M}$ ) are significantly more potent as lumazine synthase inhibitors than the next-ranking compound, the phosphonate **31c** ( $K_i$  = 130  $\mu\text{M}$ ).

It is interesting to compare the activities of the ribitylxanthine **10** ( $K_i$  470  $\mu\text{M}$ ), the corresponding ribitylazapurine **11** ( $K_i$  330  $\mu\text{M}$ ), and the ribitylpurinetrione **13** ( $K_i$  46  $\mu\text{M}$ ) versus lumazine synthase. We had previously proposed that the slightly more potent activity of **11** in comparison to **10** might reflect the possible electrostatic interaction between the positively charged Lys135 primary ammonium ion and the N-8 nitrogen of **11**, as well as a possible hydrogen bond between the Lys135 amino group and the nonbonded electron pair on

N-8 of **11**.<sup>20</sup> According to this line of reasoning, the greater potency of **13** versus **11** might reflect more favorable hydrogen bonding between the 8-keto group of **13** and the amino group of Lys135, which could also position the Lys135 amino group to participate in a second hydrogen bond with the oxygen of the 4'-hydroxyl group of the ribityl side chain (Figure 2).

It seems logical to suspect that an inhibitor of both lumazine synthase and riboflavin synthase would be a good candidate for antibiotic drug development, since resistance would be less likely to emerge against an agent that is active against more than one enzyme in the biosynthetic pathway.

## Experimental Section

**5-Ethylcarbamoyl-6-D-ribitylaminouracil (12).** A mixture of palladium on charcoal (10%, 0.3 g) in water (50 mL) was stirred in a hydrogen atmosphere for 5 min. 5-Nitro-6-D-ribitylaminouracil (**9**)<sup>21</sup> (1.0 g, 3.26 mmol) was added, and the solution was hydrogenated at room temperature and atmospheric pressure for 12 h to afford intermediate **1**. The reaction mixture was cooled to 0  $^{\circ}\text{C}$ , triethylamine (5 mL), acetonitrile (25 mL), and ethyl chloroformate (3.0 mL, 31 mmol) were added, and the mixture was stirred for 10 h. The catalyst was removed by filtration, and the filtrate was concentrated under reduced pressure. The residue was applied to a cation-exchange column (Dowex 50  $\times$  2-200, 30 g) and eluted with water (200 mL). The fractions were then applied to an anion-exchange column (Dowex 1  $\times$  2-400) and eluted with water and 10% aq HCOOH. After concentration of the combined fractions, the residue was triturated with EtOAc to generate a precipitate, which was then collected by filtration to yield **12** (0.8 g, 70%) as an amorphous solid:  $^1\text{H}$  NMR (300 MHz,  $\text{D}_2\text{O}$ )  $\delta$  4.08 (q,  $J$  = 7 Hz, 2 H), 3.81 (m, 1 H), 3.69 (m, 2 H), 3.59–3.45 (m, 3 H), 3.39 (m, 1 H), 1.17 (t,  $J$  = 7 Hz, 3 H). Anal. Calcd for  $\text{C}_{12}\text{H}_{20}\text{N}_4\text{O}_8 \cdot 1.0(\text{H}_2\text{O}) \cdot 0.2(\text{HCO}_2\text{H})$ : C, 39.41; H, 5.97; N, 14.82. Found: C, 39.33; H, 5.84; N, 14.78.

**9-D-Ribityl-1,3,7-trihydropurine-2,6,8-trione (13).** A mixture of 5-ethylcarbamoyl-6-D-ribitylaminouracil (**12**) (0.20 g, 0.57 mmol) and NaOEt (0.10 g, 1.47 mmol) in ethanol (50 mL) was heated at reflux for 24 h. After removal of the solvent under reduced pressure, the residue was purified by anion-exchange resin column chromatography (Dowex 1  $\times$  2-400, eluted with distilled water followed by 10% HCOOH) to afford **13** (120 mg, 70%) as an amorphous solid:  $[\alpha]_D^{20} +3.7^{\circ}$  (DMSO);  $^1\text{H}$  NMR (300 MHz, DMSO- $d_6$ )  $\delta$  11.50 (s, 1 H), 10.86 (s, 1 H), 10.79 (s, 1 H), 5.10–4.00 (br m, 4 H), 3.89–3.4 (m, 7 H). Anal. Calcd for  $\text{C}_{10}\text{H}_{14}\text{N}_4\text{O}_7 \cdot 2.0(\text{H}_2\text{O}) \cdot 0.5(\text{HCOOH})$ : C, 34.91; H, 5.30; N, 15.51. Found: C, 34.67; H, 5.05; N, 15.50.

**1,4-Bis[3-(5-ethylcarbamoyl-6-D-ribitylaminouracil)]-butane (17).** A suspension of palladium on charcoal (10%, 0.3 g) in water (20 mL) was stirred in a hydrogen atmosphere for 5 min. 1,4-Bis[3-(5-nitro-6-ribitylaminouracil)]butane (**15**)<sup>18</sup> (0.8 g, 1.2 mmol) and triethylamine (1 mL) were added, and the solution was hydrogenated at room temperature and atmospheric pressure for 12 h to afford intermediate **16**. The reaction mixture was cooled to 0  $^{\circ}\text{C}$ , triethylamine (1 mL), acetonitrile (5 mL), and ethyl chloroformate (1.0 mL, 11 mmol) were added, and the mixture was stirred for 10 h at room temperature. The catalyst was removed by filtration, and the filtrate was concentrated under reduced pressure. The residue was triturated with ethyl acetate to give a white precipitate, which was collected by filtration. It was dissolved in  $\text{H}_2\text{O}$  (5 mL), applied on a cation-exchange column (Dowex 50  $\times$  2-200, 20 g), and eluted with water (100 mL). After concentration of the combined fractions, the residue was triturated with  $\text{H}_2\text{O}$ /EtOH, and then collected by filtration to provide **17** (0.55 g, 61%) as an amorphous solid:  $^1\text{H}$  NMR ( $\text{D}_2\text{O}$ )  $\delta$  4.08 (q,  $J$  = 7 Hz, 4 H), 3.82 (m, 2 H), 3.7–3.5 (m, 14 H), 3.35 (m, 2 H), 1.48 (m, 4 H), 1.17 (t,  $J$  = 7 Hz, 6 H).

**1,4-Bis[1-(9-D-ribityl-1,3,7-trihydropurine-2,6,8-trionyl)]-butane (18).** Sodium (0.1 g, 4.3 mmol) was dissolved in

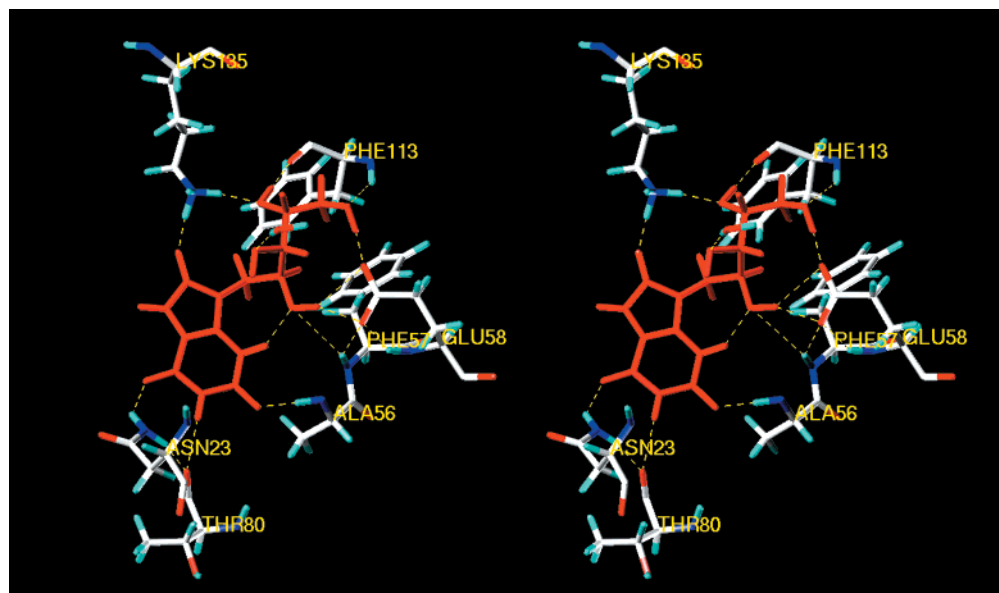


**Figure 2.** Hypothetical model for the binding of compound **13** to *B. subtilis* lumazine synthase. The figure is programmed for walled stereoviewing.

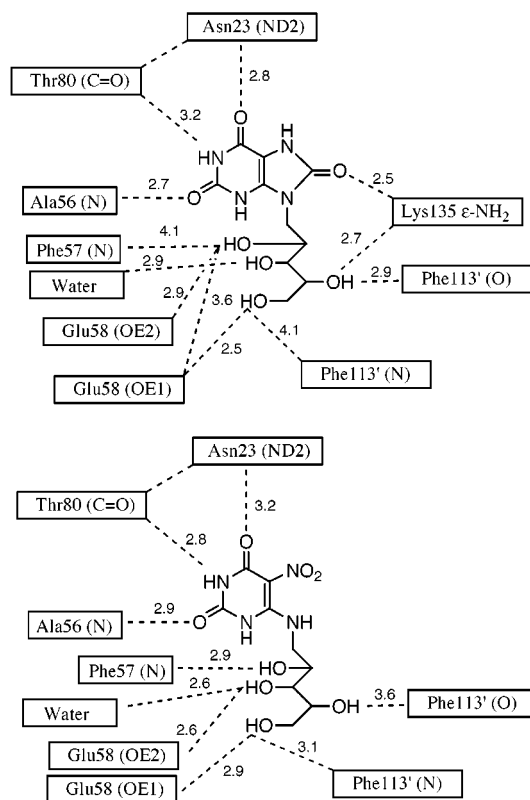


**Figure 3.** (Top) Hydrogen bonds and distances in the calculated model of the inhibitor **13** bound in the active site of *B. subtilis* lumazine synthase. (Bottom) The corresponding diagram based on the X-ray structure of the complex of **9** with the enzyme.

ethanol (60 mL). 1,4-Bis[3-(5-ethylcarbamoyl-6-D-ribitylamino-uracilyl)]butane **17** (0.10 g, 0.13 mmol) was added to the solution, and the reaction mixture was heated at reflux for 48 h. After cooling, the precipitate was collected by filtration and then purified by anion-exchange resin column chromatography (Dowex 1  $\times$  2-400, eluted with distilled water followed by 10% HCOOH) to afford **18** (50 mg, 58%) as an amorphous solid:  $^1\text{H}$  NMR (300 MHz, DMSO- $d_6$ )  $\delta$  11.8 (s, 2 H), 10.86 (s, 2 H), 5.5–4.2 (br m, 8 H), 3.85–3.0 (m, 18 H), 1.5 (m, 4 H). Anal.

Calcd for  $\text{C}_{24}\text{H}_{34}\text{N}_8\text{O}_{14} \cdot 2.6(\text{H}_2\text{O})$ : C, 40.86; H, 5.60; N, 15.88. Found: C, 40.86; H, 5.32; N, 15.62.

**Molecular Modeling.** Using Sybyl (Tripos, Inc., version 6.5, 1998), the X-ray crystal structure of the complex of 5-nitro-6-ribitylamino-2,4-(1*H*,3*H*)pyrimidinedione (**9**) and the heavy riboflavin synthase of *B. subtilis* (1RVV)<sup>7</sup> was clipped to include information within a 15 Å sphere of one of the 60 equivalent ligand molecules. The residues that were clipped in this cut complex were capped with either neutral amino or carboxyl groups. The structure of the inhibitor **13** was overlapped with the structure of 5-nitro-6-ribitylamino-2,4-(1*H*,3*H*)pyrimidinedione (**9**), which was then deleted. Hydrogen atoms were added to the complex. MMFF94 charges were loaded, and the energy of the complex was minimized using the Powell method to a termination gradient of 0.05 kcal/mol while employing the MMFF94 force field. During the minimization of the complex, inhibitor **13** and a 6 Å sphere surrounding it were allowed to remain flexible, while the remaining portion of the complex was held rigid using the aggregate function. Figure 2 was constructed by displaying the amino acid residues of the enzyme and one water molecule that are calculated to be involved in hydrogen bonding with the inhibitor **13**. The maximum distance of the hydrogen bonds shown in Figure 2 was set at 3.4 Å.

**Lumazine Synthase Assay.**<sup>26</sup> Reaction mixtures contained 100 mM potassium phosphate, pH 7.0, 5 mM EDTA, 5 mM dithiothreitol, inhibitor (0–862  $\mu\text{M}$ ), 153  $\mu\text{M}$  5-amino-6-ribitylamino-2,4(1*H*,3*H*)-pyrimidinedione (**1**), and recombinant *B. subtilis* lumazine synthase capsids (30  $\mu\text{g}$ , specific activity 12.5  $\mu\text{mol mg}^{-1} \text{h}^{-1}$ ) in a total volume of 560  $\mu\text{L}$ . The solution was incubated at 37  $^\circ\text{C}$ , and the reaction was started by the addition of a small volume (20  $\mu\text{L}$ ) of L-3,4-dihydroxy-2-butanone 4-phosphate to a final concentration of 17–166  $\mu\text{M}$ . The velocity/substrate data were fitted for all inhibitor concentrations with a nonlinear regression method using the program DynaFit.<sup>27</sup> Different inhibition models were considered for the calculation.  $K_i$  values  $\pm$  standard deviations were obtained from the fit under consideration of the most likely inhibition model.

**Riboflavin Synthase Assay.**<sup>28</sup> Reaction mixtures contained buffer (100 mM potassium phosphate, 10 mM EDTA, 10 mM sodium sulfite), inhibitor (0–40  $\mu\text{M}$ ), and *E. coli*

(26) Kis, K.; Bacher, A. *J. Biol. Chem.* **1995**, *270*, 16788–16795.

(27) Kuzmic, P. *Anal. Biochem.* **1996**, *237*, 260–273.

(28) Eberhardt, S.; Richter, G.; Gimbel, W.; Werner, T.; Bacher, A. *Eur. J. Biochem.* **1996**, *242*, 712–718.

riboflavin synthase (10  $\mu$ g, specific activity 50  $\mu$ mol  $\text{mg}^{-1}$   $\text{h}^{-1}$ ). After preincubation, the reactions were started by the addition of various amounts of 6,7-dimethyl-8-ribityllumazine (**3**) (16–166  $\mu$ M) to a total volume of 620  $\mu$ L. The formation of riboflavin (**4**) was measured online with a computer-controlled photometer at 470 nm ( $\epsilon_{\text{riboflavin}} = 9100 \text{ M}^{-1} \text{ cm}^{-1}$ ). The  $K_i$  evaluation was performed in the same manner as described above.

**Acknowledgment.** This research was made possible by NIH grant GM51469 and by support from the Deutsche Forschungsgemeinschaft and Fonds der Chemischen Industrie.

JO010706R